

# Electrochemical behaviour of Al–In alloys in chloride solutions

S. B. SAIDMAN, S. G. GARCIA, J. B. BESSONE

*Instituto de Ingeniería Electroquímica y Corrosión (INIEC),  
Departamento de Química e Ingeniería Química, Universidad Nacional del Sur, Av. Alem 1253,  
8000 Bahía Blanca, República Argentina*

Received 10 June 1993; revised 13 September 1993

The present work is concerned with the study of the activation mechanism of Al in alloys produced by indium. The electrochemical behaviour of aluminium in NaCl solutions containing  $\text{In}^{3+}$  ions and the dissolution of Al–In and In–Al alloys were studied using potentiostatic, galvanostatic and potentiodynamic techniques, complemented by SEM. It was concluded that the aluminium activation is obtained only when indium comes into a true metallic contact with aluminium within an active pit and in the presence of chloride ions. Polarization curves for dissolution of Al–In and In–Al alloys were compared. The results suggest that the initial step in the dissolution mechanism of the Al–In alloy can be interpreted through chloride ion adsorption on a surface In–Al alloy. This adsorption occurs at more electronegative potentials than that of pure aluminium, thus avoiding repassivation.

## 1. Introduction

Electrochemical studies of aluminium alloys have been mainly motivated by the application of these alloys in Al–battery systems and as anode materials in cathodic protection systems. Most sacrificial anodes used worldwide are consumed in protecting steel structures in sea water. Pure aluminium supports a thin protective oxide film on the surface with an operational potential in sea water of approximately  $-0.800\text{ V}$  [1], which makes it useless as a pure metal sacrificial anode. Nevertheless, aluminium is a material that may be used as a sacrificial anode by adding suitable alloying elements. It has long been known that some elements will depassivate the oxide film on aluminium. Reading and Newport [2] have examined a total of some 2 500 aluminium alloys, binary and ternary compositions, in artificial sea water. They observed that five elements, In, Hg, Sn, Ga and Bi lowered the operating potential by more than  $0.3\text{ V}$  compared with that of pure aluminium, while Zn, Cd, Mg and Ba lowered it by  $0.1$  to  $0.3\text{ V}$ . These results formed the basis for most of the subsequent anode alloy development work.

Specifically, the performance of Al–Zn–In alloy as a sacrificial anode is of interest from a theoretical, as well as an applied, point of view. A better knowledge of the behaviour of the binary and primary components is required. It has been demonstrated that aluminium is activated, not only when alloyed with In metal [3, 4], but also when placed in neutral solutions containing indium ions [5–7]. However, the mechanism by which In exerts its activation effect on aluminium is still not well understood. Therefore, this study was carried out

on the electrochemical behaviour of aluminium in NaCl solutions containing  $\text{In}^{3+}$  ions, and Al–In and In–Al alloys in NaCl solutions.

## 2. Experimental details

The binary alloys were prepared with different nominal compositions (Al–0.02%In; Al–0.09%In; Al–5%In; In–1.7%Al; In–5%Al), from pure elements (Al 99.99 wt %; In 99.999 wt %). These elements were placed in a cylindrical graphite crucible located in a stainless steel crucible, and supported between two copper plates, attached to a mechanical vibrator. The copper plates and the crucibles were heated resistively to raise the temperature of the alloy to  $850^\circ\text{C}$ . The system was shaken for 1 min and allowed to rest for 2 min; the procedure was repeated for approximately 25 minutes. The crucible was then cooled at room temperature. All alloys were used as-cast, and electrodes were obtained from the binary ingots. Due to the extremely low solid solubility of indium in aluminium and vice versa, a second phase in the system is expected, instead of one simple solid solution. Nevertheless, the term alloy will be used to identify these systems.

Pure aluminium and binary alloy discs, axially mounted in a PTFE holder, were used as working electrodes. Each electrode was polished successively with 400, 600 and 1200 grade emery paper,  $1\ \mu\text{m}$  and  $0.3\ \mu\text{m}$  grit alumina suspension and then thoroughly rinsed with thrice distilled water. The auxiliary electrode was a large area platinum sheet separated from the main electrolyte compartment by a sintered glass diaphragm. Potentials were measured against a properly shielded SCE and connected through a Luggin–Haber capillary tip.

All potentials in this work are referred to the SCE scale.

The cell used in the experiments was a conventional three compartment Pyrex glass cell kept at  $25 \pm 0.1^\circ\text{C}$  with a Colora Ultra Thermostat NB. The instruments used for the electrochemical measurements were a linear voltage sweep generator (PAR Model 175), a potentiostat/galvanostat (PAR model 173), an X-Y recorder (HP 4007 B) and a millivoltmeter (Knick model 35). A dual stage ISI DS 130 SEM and an EDAX 9600 quantitative energy dispersive analyser were used to examine the electrode attack.

Potentiostatic, potentiodynamic and galvanostatic experiments were carried out on the alloys in  $x\text{M}$  NaCl solutions ( $0.001 \leq x \leq 2$ ).

The indium decoration process [8] was studied at different galvanostatic conditions by immersing an aluminium specimen in a  $y\text{M}$   $\text{In}_2(\text{SO}_4)_3$  ( $0.01 \leq y \leq 0.1$ ) solution with and without chloride presence.

### 3. Results and discussion

#### 3.1. Effects of $\text{In}^{3+}$ and $\text{Cl}^-$ ions on the Al activation process

When aluminium supporting an air-formed oxide is placed in a solution containing  $\text{In}^{3+}$  ions, an indium decoration process takes place. It is possible to displace  $\text{In}^{3+}$  ions from the solution by the galvanic action produced by the electrooxidation of bare aluminium transiently revealed at the oxide cracked flaws which tend to repassivate [9]. This displacement reaction produces tiny indium particles reduced at cathodic sites revealing the presence of local favourably electronically conducting regions on the specimen surface. These cathodic bridges are mainly given by cathodic impurities normally present in the pure aluminium matrix, such as Cu, Fe or Si.

Two aluminium specimens were decorated for 10 min in a  $0.1\text{M}$   $\text{In}_2(\text{SO}_4)_3$  solution in an open circuit condition. Both specimens were then immersed

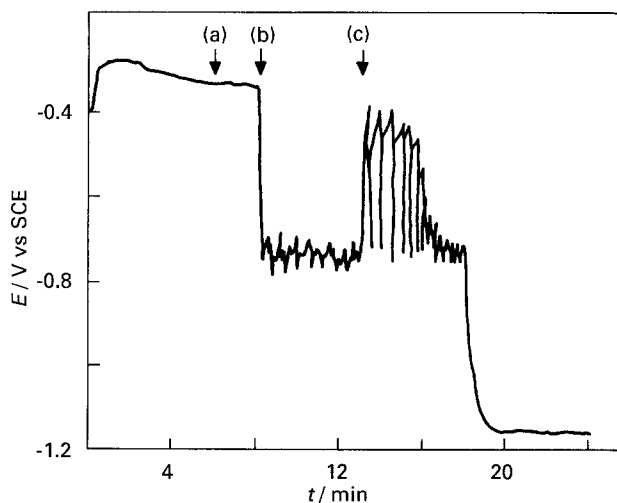


Fig. 1. Combined effect of  $\text{Cl}^-$  and  $\text{In}^{3+}$  ions. Initial system: Al/In decorated in distilled water. Additions: (a) Twice distilled water washing; (b)  $0.5\text{M}$  NaCl; (c)  $25\text{ ml}$   $0.1\text{M}$   $\text{In}_2(\text{SO}_4)_3$ .

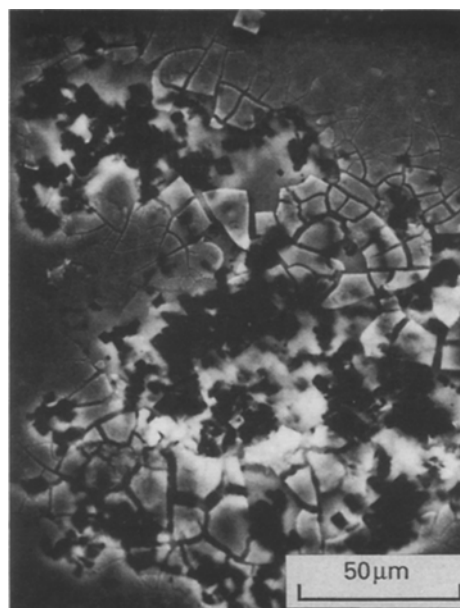


Fig. 2. SEM micrograph ( $2.6\text{K}\times$ ) of aluminium crystallographic attack, after decoration for 10 min in a  $0.1\text{M}$   $\text{In}_2(\text{SO}_4)_3$  solution, twice washed with distilled water and immersed in a  $0.5\text{M}$  NaCl solution for 5 min.

in distilled water (pH 5.7) where their  $E/t$  response was followed during the first 10 min (Fig. 1). The volume of solution ( $100\text{ cm}^3$ ) was then replaced twice by fresh distilled water to avoid the presence of  $\text{In}^{3+}$  ions. At this stage the potential measured was  $-0.340\text{ V}$ . Here, in spite of being an electropolished aluminium specimen in distilled water, a relatively noble corrosion potential was developed. This effect is produced by the decorated indium particles, which have considerably increased the available cathodic areas, favouring the anodic polarization of the whole specimen by the  $\text{O}_2/\text{OH}^-$  couple.

After washing in distilled water, NaCl was added to give a  $0.5\text{M}$  solution. The corrosion potential dropped rapidly to approximately  $-0.740\text{ V}$ , where

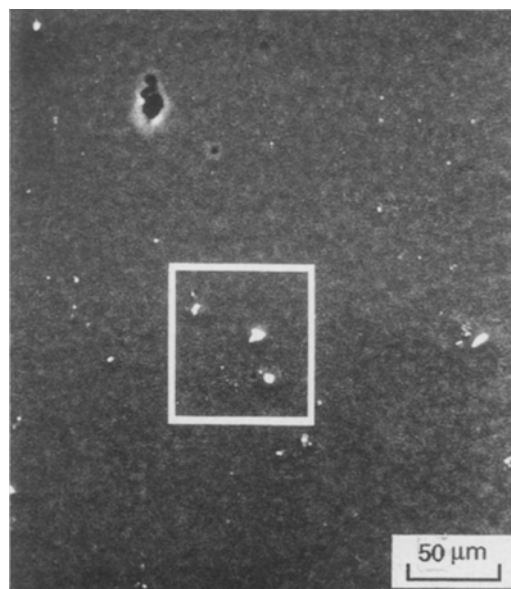


Fig. 3. SEM micrograph ( $310\times$ ) of an aluminium specimen after decoration for 10 min in a  $0.1\text{M}$   $\text{In}_2(\text{SO}_4)_3$  solution, twice washed with distilled water and immersed in a  $0.5\text{M}$  NaCl solution for 5 min. Indium deposits were detected in the marked area.

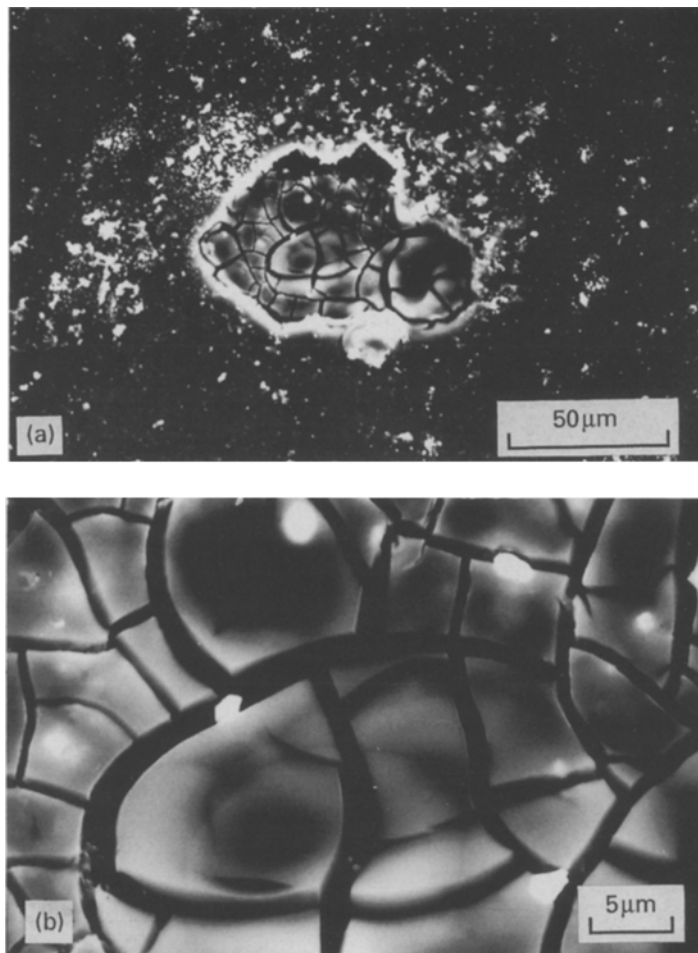


Fig. 4. (a) and (b) SEM micrographs obtained at different magnifications of an aluminium specimen after attack for 35 min in 0.5 M NaCl + 0.025 M  $\text{In}_2(\text{SO}_4)_3$ . (b) Shows the mud cake structured film inside the cavity and the particles within.

it remained, fluctuating with an amplitude of approximately 0.050 V. Under this experimental condition (the  $\text{O}_2/\text{OH}^-$  couple polarizes the specimen), this corrosion potential is the pitting potential of pure aluminium in a 0.5 M NaCl solution [10]. Five minutes after the chloride addition, one specimen was removed and examined by SEM. Figure 2 shows the presence of crystallographic pits with no In deposit within or around them. In particles produced by the initial decoration, identified by X-ray mapping (Fig. 3), were found at positions far from the pits. These results suggest that no influence was exerted by In in the activation process, when indium is merely present on the oxide film as a reduced particle.

The experiment was continued by adding 25 ml of 0.1 M  $\text{In}_2(\text{SO}_4)_3$  to the chloride solution where the

other specimen still remained pitting. The corrosion potential began to fluctuate with an initial amplitude of about 0.400 V, and a relatively low frequency. Afterwards, the amplitude of the potential surges decreased while the frequency increased. After approximately 5 min, the corrosion potential was shifted to  $-1.160$  V denoting a further activation of the specimen, and it remained at that potential for a further 30 min with no appreciable potential surges. Without washing, the specimen was examined by SEM. The attacked areas showed wide cavities (Fig. 4(a)). At higher magnification, the corrosion product within the pit presented a mud-crack structure (Fig. 4(b)). The high chloride concentration detected by the X-ray map (Fig. 5) suggests the presence of a salt film. Indium particles within and

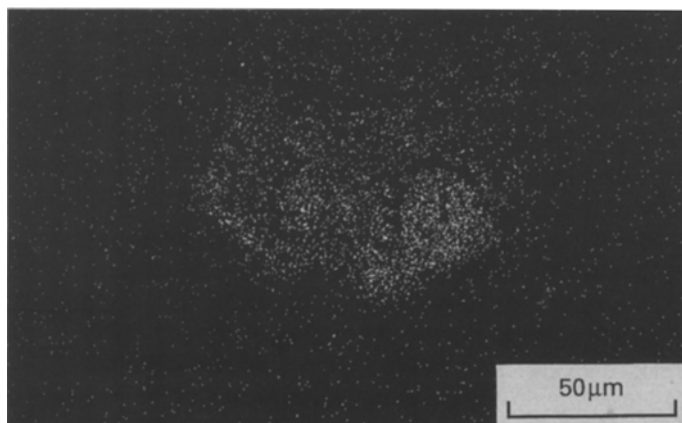


Fig. 5.  $\text{Cl K}_\alpha$  X-ray map on plate in Fig. 4(a).

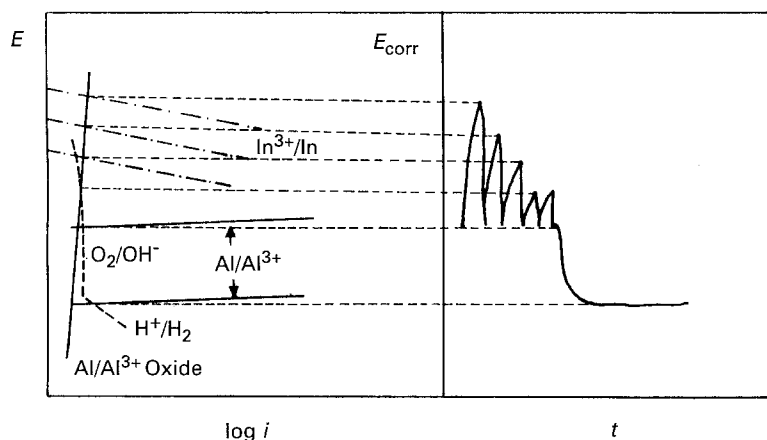


Fig. 6. Schematic representation of the  $E_{\text{corr}}/t$  behaviour found in Fig. 1.

above the salt film may be seen in Fig. 4(b), identified by X-ray map.

It is possible to explain the potential fluctuations observed after the addition of  $\text{In}^{3+}$  ions to the chloride solution. At this stage, the aluminium specimen is already pitted and  $\text{In}^{3+}$  ions can be reduced inside the pits as well as outside. The process is represented schematically in Fig. 6. The  $\text{In}/\text{In}^{3+}$  couple polarizes the whole system (upper limit of the potential fluctuations). This polarization is interrupted when a new oxide crack is produced, transiently revealing bare aluminium and shifting the potential towards negative values (lower limit of the fluctuations). This potential is defined by the  $\text{Cl}^-$  ion adsorption potential on the bare aluminium [11, 12]. This active state consumes  $\text{In}^{3+}$  ions by reducing them on the bare aluminium, diminishing the amplitude of the potential fluctuations.

At this point, the presence of  $\text{Cl}^-$  ions may be sustained by a new active surface, where In was reduced, at a more negative potential ( $-1.160\text{ V}$ ). No appreciable potential fluctuations were observed at this stage, which suggest that strong  $\text{Cl}^-$  adsorption maintains this active state. According to Rotenberg and Pleskov [13], the  $E_{\text{pzc}}$  for indium metal in  $10^{-2}\text{ M}$  KCl containing  $10^{-3}\text{ M}$  HCl is  $-0.9\text{ V}$ . Furthermore, the chloride concentration is strongly increased in the pitted areas due to migration, and combining this with the high affinity of In for  $\text{Cl}^-$ , as suggested by Carroll and Breslin [7], this gives rise to a high surface concentration of  $\text{Cl}^-$ . Therefore, it is expected that  $\text{Cl}^-$  adsorption takes place at a much more electronegative potential ( $-1.160\text{ V}$ ). This effect, and the subsequent aluminium dissolution, produced the salt film observed in Fig. 4. The attacked morphology has changed, as can be seen by comparing Fig. 2 with Fig. 4(a), where this process is still in progress. The initial crystallographic attack developed on pure aluminium is being transformed into wide cavities. A characteristic feature of the aluminium base alloy containing indium is to give a relatively smooth surface attack [14]. This effect can be ascribed to the presence of a salt film. Vetter [15] proposed that a salt layer ( $\text{AlCl}_3$ ) is responsible for a hemispherical shape with smooth surface, produced by the resistance polarization given by a nonohmic potential drop in a solid salt

film. This film causes a homogeneous current distribution with a role similar to the well known electropolishing layer, which brightens the surface of the specimen.

In these working conditions, it is possible to displace  $\text{In}^{3+}$  ions from the solution by the galvanic action produced by the aluminium oxidation process. The results suggest that the aluminium activation is reached only when the indium decoration process takes place within an active pit, producing a true In/Al metallic contact. If decoration occurs on the oxide, no activation is observed. The aluminium activation is also achieved when an indium particle is mechanically attached to the aluminium surface. Furthermore, the experiments demonstrated that the presence of indium in contact with bare aluminium does not produce activation *per se*. Indium avoids repassivation only in the presence of chloride ions.

The effects of indium on the activation process of aluminium in the presence of  $\text{Cl}^-$  ions, was also studied using a galvanostatic/potentiodynamic technique. First, aluminium was attacked in a  $0.5\text{ M}$  NaCl solution applying for 5 min a galvanostatic anodic c.d. of  $1\text{ mA cm}^{-2}$ . Although pitting propagation initially changes the electrode active area, the current applied is given as a c.d. referred to the initial electrode geometric area for comparison reasons. Immediately after, the electrode was immersed in a  $x\text{ M}$  NaCl +  $0.01\text{ M}$   $\text{In}_2(\text{SO}_4)_3$  solution ( $0.1 < x < 2$ ) and a galvanostatic anodic c.d. of  $1\text{ mA cm}^{-2}$  was applied again for 5 min. The potential shifted to  $-1.165$ ,  $-1.140$  and  $-1.110\text{ V}$  for  $x = 2, 1$  and  $0.5\text{ M}$  NaCl, respectively. This effect was due to the  $\text{In}^{3+}$  ions galvanically reduced on the reactive areas present within the pits. When the aluminium electrode was immersed in  $0.1\text{ M}$  NaCl +  $0.01\text{ M}$   $\text{In}_2(\text{SO}_4)_3$ , the potential shifted from  $-0.870$  to  $-0.690\text{ V}$ . This shows that the chloride ion concentration ( $C_{\text{Cl}^-} \leq 0.1\text{ M}$ ) is insufficient to maintain an active state. The existence of a synergistic effect between In and chloride ions has previously been observed [7]. This effect may be explained considering that, for decreasing chloride ion concentration, the pitting potential of aluminium increases and the deposition rate of indium on the surface diminishes.

After reaching the active state in the  $x\text{ M}$  NaCl+

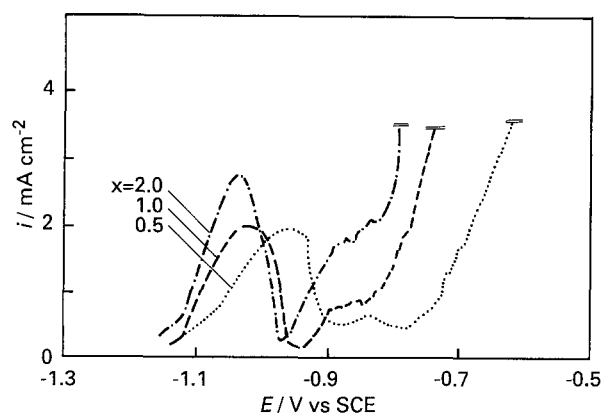


Fig. 7.  $i/E$  profiles of aluminium electrodes in  $xM$   $\text{NaCl} + 0.01M$   $\text{In}_2(\text{SO}_4)_3$  at  $v = 0.001 \text{ V s}^{-1}$ . The specimens were previously activated for 5 min at c.d.  $1 \text{ mA cm}^{-2}$  in the same solution.

$0.01M$   $\text{In}_2(\text{SO}_4)_3$  solution under the galvanostatic mode, the polarization mode was changed to a potentiostatic one and the aluminium electrode was now polarized potentiodynamically in the positive potential direction at  $0.001 \text{ V s}^{-1}$  (Fig. 7). The polarization curves initially show an activation process, which was affected by the chloride ion concentration. Afterwards the current decreases, denoting a repassivation to give finally a sharp increase in the anodic current, at more positive potential, due to pitting of the aluminium matrix. The voltammetric response found for pure In in chloride solution [16] shows an anodic peak, which does not depend on chloride concentration, but is associated with the electroformation of a hydroxide/oxide film. On the contrary, the activation process in Fig. 7 shifts to more electronegative potentials as the chloride concentration increases. Probably, the electrooxidation of a phase, where indium and aluminium are present, takes place in this potential range and a strong  $\text{Cl}^-$  adsorption process is initially needed to produce it. It will be shown later, that a similar response is given by an In-Al alloy. On the other hand, once the anodic current dissolves the surface phase formed by the previous In reduction, as well as the aluminium matrix which surrounds it, the active state vanishes and repassivation follows.

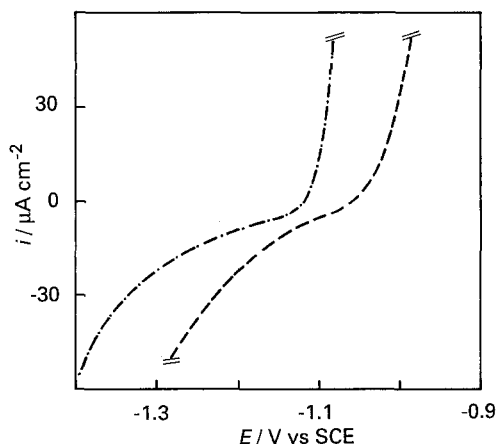


Fig. 8. The polarization behaviour of Al-In alloys in a  $0.5M$   $\text{NaCl}$  solution. Scan rate used was  $0.001 \text{ V s}^{-1}$  initiated at  $-1.4 \text{ V}$  vs SCE. (---) Al-0.09%In, (- · - ·) Al-5%In.

Table 1. Corrosion potentials of Al-5%In and Al-0.09%In alloys at different chloride concentrations

$C_{\text{Cl}^-}/M$	$E_{\text{corr}}/V$	
	Al-5%In	Al-0.09%In
0.05	-1.033	-1.020
0.10	-1.110	-1.100
0.50	-1.150	-1.130
1.00	-1.250	-1.235

### 3.2. Al-In and In-Al alloys

The present work also includes studies of the influence of indium concentration on the electrochemical behaviour of Al-In alloys. Figure 8 shows the polarization curves at a scan rate of  $0.001 \text{ V s}^{-1}$  for Al-0.09%In and Al-5%In alloys in  $0.5M$   $\text{NaCl}$  solution. A sharp increase in current was observed starting at  $-1.050$  and  $-1.125 \text{ V}$  (breakdown potential,  $E_b$ ), respectively, associated with a pitting process detected by microscopic observation. The same process started at  $-0.730 \text{ V}$  for the Al-0.02% indium alloy, although current oscillations were registered starting from  $-1.050 \text{ V}$ .

The corrosion potentials measured at different chloride concentrations are listed in Table 1. Again, under the experimental conditions used, these corrosion potentials obtained at open circuit, are equivalent to their pitting potentials ( $E_b$ ).

Further details of the entire process can be obtained by analyzing the  $E$  against  $t$  potential transient when a current step of  $1 \text{ mA cm}^{-2}$  is applied to an Al-In alloy in a chloride solution (Fig. 9). Different values of  $E_{\text{corr}}$  ( $= E_b$ ),  $E_{\text{ss}}$ ,  $E_{\text{max}}$  and  $t$  are obtained for different In percentages in the alloy (Table 2), where:

- $E_{\text{corr}}$  corrosion potential measured at the beginning of the experiment
- $E_{\text{ss}}$  steady state potential at  $i = 1 \text{ mA cm}^{-2}$
- $E_{\text{max}}$  maximum potential registered at  $i = 1 \text{ mA cm}^{-2}$
- $t$  time elapsed to attain  $E_{\text{ss}}$ .

To obtain more information about the electrochemical behaviour of Al-In alloys, the polarization curves of In-Al alloys in chloride solution at  $0.001 \text{ V s}^{-1}$  were measured. The electrochemical  $i/E$  response of In-5%Al exhibits an anodic peak (A) followed by a current plateau (Fig. 10). Current oscillations appear for potentials higher than  $E_{p,A}$ . Finally, when the potential exceeds  $E_b$ , there is a sharp increase in the anodic current. Table 3 shows

Table 2. Variation of  $E_{\text{corr}}$ ,  $E_{\text{ss}}$ ,  $E_{\text{max}}$  and  $t$  for different indium percentages present in the alloy

$x\% \text{In}$	$E_{\text{corr}}/V$	$E_{\text{ss}}/V$	$E_{\text{max}}/V$	$t/s$
5.00	-1.150	-1.100	-0.870	6
0.09	-1.150	-1.070	-0.700	15
0.02	-0.860	-0.856	-0.680	27
0	-0.780	-0.730	-0.690	0.15

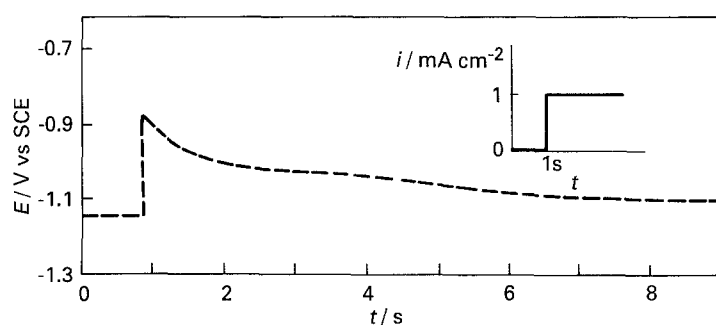


Fig. 9.  $E$  against  $t$  plot obtained for the Al-5%In alloy in a 0.5 M NaCl after applying the perturbation programme shown in the Figure.

the initial potential of peak A ( $E_{in}$ ),  $E_{p,A}$  and  $E_b$  measured for In-5%Al at different chloride concentrations. The anodic charge recorded up to the peak potential is practically independent of the chloride concentration ( $5 \text{ mC cm}^{-2}$ ). The  $i/E$  curve does not change significantly for In-1.7%Al.

The results suggest that the electrodisolution of In-Al alloys, associated with peak A, is assisted by the presence of chloride. The initial potential of peak A ( $E_{in}$ ) for In-Al alloys at chloride concentrations  $0.05 \text{ M} \leq C_{Cl^-} \leq 1 \text{ M}$  (Table 3) is very close to the corrosion potentials ( $E_{corr} = E_b$ ) for Al-In alloys (Table 1). This agreement may be explained considering that the chloride adsorption on In-Al (formed in the Al-In matrix) initiates the anodic dissolution. The formation of surface Ga-Al in Al-Ga alloys has been proposed by Tyck *et al.* [17]. For the Al-0.02%In alloy, current oscillations were found to initiate at potentials very close to the  $E_{in}$  for In-Al alloys. These oscillations are produced by aluminium oxide disruptions where local aluminium dissolution increases the amount of In-Al alloy thus increasing the anodic current, which tends to repassivate the oxide break.

When a galvanostatic step of  $1 \text{ mA cm}^{-2}$  is applied, the electrode potential of Al-In alloy is initially shifted to a value which probably tends to the Al/ $\text{Al}^{3+}$  potential, and then relaxes to attain a steady

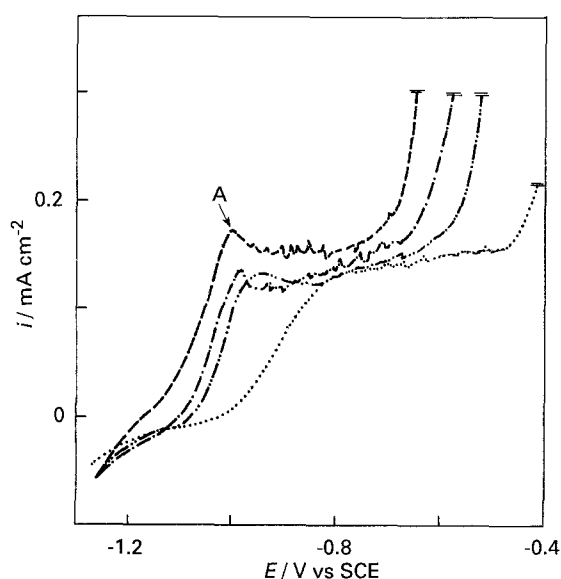


Fig. 10. Influence of the NaCl concentration on the polarization behaviour of In-5%Al alloy. Scan rate used was  $0.001 \text{ V s}^{-1}$  initiated at  $-1.25 \text{ V}$ .  $y/\text{M NaCl}$ : (---) 1; (-·-·-) 0.5; (-·-·-·) 0.1; (·····) 0.01.

state potential. The time necessary to reach  $E_{ss}$  increases as the indium concentration in the alloy decreases. This time is related to the time necessary to accumulate a minimum amount of In-Al phase concentration. The dissolution of aluminium leaves an accumulation of the indium component on the surface [4], and the initial dissolution of the Al-In alloy also favours a local In enrichment due to its reduction. On the other hand, the corrosion of aluminium is an exothermic reaction and the temperature of the electrolyte was often found to be higher than the ambient temperature [3], and this may produce a surface temperature high enough to promote the In-Al phase formation. Comparing the three systems already analysed (Figs 7, 8 and 10) indicates a similar activation process, where the active mass is mainly given by aluminium. Each of these systems involves a different amount of the active and chloride sensitive reactive phase. The common factor which possibly relates their activation process is the formation of a surface In-Al alloy.

#### 4. Conclusion

The most important conclusions reached in this study are as follows:

- (i) Aluminium activation is obtained only when the indium decoration process takes place within an active pit, producing a true In/Al metallic contact.
- (ii) Indium prevents aluminium repassivation at very electronegative potentials only in the presence of chloride ions. Indium in contact with bare aluminium does not produce activation *per se*.
- (iii) A minimum  $\text{Cl}^-$  ion concentration is necessary to produce the activation process for a constant  $\text{In}^{3+}$  ion concentration, and vice versa.
- (iv) It is suggested that the formation of a surface In-Al alloy is responsible for  $\text{Cl}^-$  ion adsorption at more electronegative potentials than aluminium,

Table 3. Variation of the initial potential of peak A ( $E_{in}$ ),  $E_{p,A}$  and  $E_b$  obtained for In-5%Al at different chloride concentrations

$C_{Cl^-}/\text{M}$	$E_{in}/\text{V}$	$E_{p,A}/\text{V}$	$E_b/\text{V}$
1.00	-1.175	-1.010	-0.750
0.50	-1.120	-0.985	-0.700
0.10	-1.090	-0.950	-0.650
0.01	-1.040	—	-0.500

thus preventing aluminium repassivation. Further experimental work is now in progress.

### Acknowledgements

This research was financially supported by the Universidad Nacional del Sur (UNS), the Consejo Nacional de Investigaciones Cientificas y Técnicas (CONICET, PID No. 311 070 088) and the Volkswagenwerk, Stiftung (Germany).

### References

- [1] B. M. Ponchel and R. L. Horst, *Mater. Protection* **7** (1968) 38.
- [2] J. T. Reading and J. J. Newport, *ibid.* **5** (1966) 15.
- [3] W. Wilhelmsen, T. Arnesen, Ø. Hasvold and N. J. Størkersen, *Electrochim. Acta* **36** (1991) 79.
- [4] L. Bai and B. E. Conway, *J. Appl. Electrochem.* **22** (1992) 131.
- [5] M. C. Reboul, Ph. Gimenez and J. J. Rameau, *Corrosion* **40** (1984) 366.
- [6] G. Burri, W. Luedi and O. Haas, *J. Electrochem. Soc.* **136** (1989) 2167.
- [7] W. M. Carroll and C. B. Breslin, *Corros. Sci.* **33** (1992) 1161.
- [8] J. A. Richardson, G. C. Wood and W. H. Sutton, *Thin Solid Films* **16** (1973) 99.
- [9] J. B. Bessone, PhD thesis, UMIST, Manchester, UK (1983).
- [10] J. R. Galvele, 4th Int. Symp. on Passivity, Airlie, VA, USA, Oct. (1977).
- [11] YA M. Kolotyркиn, *Corrosion* **19** (1963) 261 t.
- [12] G. Sussek, M. Kesten and H. G. Feller, *Metall.* **33** (1979) 1031.
- [13] Z. A. Rotenberg and Yu. V. Pleskov, *Elektrokhimiya* **9** (1973) 1419.
- [14] J. B. Bessone, R. A. Suárez Baldo and S. M. de De Micheli, *Corrosion* **37** (1981) 533.
- [15] K. J. Vetter, Proc. Conf. on Passivity and its Breakdown on Iron and Iron Base Alloys (edited by R. W. Stahele and H. Okada), NACE VI (1976) p. 332.
- [16] S. B. Saidman and J. B. Bessone, *Electrochim. Acta* **36** (1991) 2063.
- [17] C. D. S. Tyck, J. A. Hunter and G. M. Scamans, *J. Electrochem. Soc.* **134** (1987) 2970.